

# Insights into the molecular interactions between aminopeptidase and amyloid beta peptide using molecular modeling techniques

Maruti J. Dhanavade · Kailas D. Sonawane

Received: 27 November 2013 / Accepted: 31 March 2014 / Published online: 12 April 2014  
© Springer-Verlag Wien 2014

**Abstract** Amyloid beta (A $\beta$ ) peptides play a central role in the pathogenesis of Alzheimer's disease. The accumulation of A $\beta$  peptides in AD brain was caused due to overproduction or insufficient clearance and defects in the proteolytic degradation of A $\beta$  peptides. Hence, A $\beta$  peptide degradation could be a promising therapeutic approach in AD treatment. Recent experimental report suggests that aminopeptidase from *Streptomyces griseus* KK565 (SGAK) can degrade A $\beta$  peptides but the interactive residues are yet to be known in detail at the atomic level. Hence, we developed the three-dimensional model of aminopeptidase (SGAK) using SWISS-MODEL, Geno3D and MODELLER. Model built by MODELLER was used for further studies. Molecular docking was performed between aminopeptidase (SGAK) with wild-type and mutated A $\beta$  peptides. The docked complex of aminopeptidase (SGAK) and wild-type A $\beta$  peptide (1IYT.pdb) shows more stability than the other complexes. Molecular docking and MD simulation results revealed that the residues His93, Asp105, Glu139, Glu140, Asp168 and His255 are involved in the hydrogen bonding with A $\beta$  peptide and zinc ions. The interactions between carboxyl oxygen atoms of Glu139 of aminopeptidase (SGAK) with water molecule

suggest that the Glu139 may be involved in the nucleophilic attack on Ala2–Glu3 peptide bond of A $\beta$  peptide. Hence, amino acid Glu139 of aminopeptidase (SGAK) might play an important role to degrade A $\beta$  peptides, a causative agent of Alzheimer's disease.

**Keywords** Alzheimer's disease · Amyloid beta (A $\beta$ ) · Aminopeptidases (APNs) · Molecular docking and MD simulations

## Abbreviations

AD	Alzheimer's disease
A $\beta$ peptide	Amyloid beta peptide
SGAK	Aminopeptidase from <i>Streptomyces griseus</i> strain KK565
MD	Molecular dynamics
RMSD	Root mean square deviation

## Introduction

Aminopeptidases (APNs) are zinc-dependent enzymes which cleave peptides from amino terminal end (Taylor 1993a, b; Yao and Cohen 1999). They are classified by various ways such as number of amino acids cleaved from NH<sub>2</sub>-terminus, relative efficiency of removing residues, location, susceptibility to inhibitors, metal ion content, residues that coordinated the metal ion to the enzyme, and pH for their maximal activity, etc (Lendeckel et al. 2000). Aminopeptidases are involved in numerous functions such as activation, modulation, and degradation of bioactive peptides (Stoltze et al. 2000; Hui 2007). These enzymes are widely distributed among bacteria and can be expressed as

**Electronic supplementary material** The online version of this article (doi:10.1007/s00726-014-1740-0) contains supplementary material, which is available to authorized users.

M. J. Dhanavade · K. D. Sonawane  
Department of Microbiology, Shivaji University,  
Kolhapur 416004, Maharashtra, India

K. D. Sonawane (✉)  
Structural Bioinformatics Unit, Department of Biochemistry,  
Shivaji University, Kolhapur 416 004, Maharashtra, India  
e-mail: kds\_biochem@unishivaji.ac.in

membrane or cytosolic proteins, or secreted from the cell (Gonzales and Robert-Baudouy 1996). The basic function of bacterial APNs is to digest amino acids at the N-terminus of peptides derived from the extracellular as well as intracellular environment (Gonzales and Robert-Baudouy 1996). This degradation process of peptides may be accomplished by digestion with different APNs (Miller and Green 1983), which can be important during bacterial starvation (Reeve et al. 1984). It has been reported that the aminopeptidase can cleave A $\beta$  peptides, a causative agent of Alzheimer's disease (Yoo et al. 2010).

Alzheimer's disease (AD) is the most common form of dementia in elderly. AD is mainly characterized by neurofibrillary tangles (NFTs) and senile plaques. These senile plaques are extracellular deposits composed of aggregated peptides called A $\beta$  (Selkoe 1991). The proteolytic action of both  $\beta$ - and  $\gamma$ -secretase results in the A $\beta$  peptide formation which is then secreted into the extracellular milieu (Selkoe 2004; Haass and Selkoe 2007; Selkoe and Wolfe 2007). The A $\beta$  peptide accumulation was caused due to overproduction or inefficient clearance and defects in the proteolytic degradation (Tanzi et al. 2004). Therefore, A $\beta$  degradation and clearance could be a promising therapeutic approach in AD treatment. The regulation of A $\beta$  peptides by proteolysis has significant implications in pathogenesis and in the AD treatment (Sarah et al. 2006). In addition to this, AD is characterized by the deposition of complex sets of A $\beta$ -related fragments with various N- and C-terminal ends (Iwatsubo et al. 1996). The N-terminally truncated A $\beta$  (1–42) peptides were detected in the diffused plaques at an early stage of the pathology (Iwatsubo et al. 1996). However, N-terminal heterogeneity has been observed in parenchymal and cerebrovascular A $\beta$  deposits (Tekirian et al. 1998; Thal et al. 1999; Takeda et al. 2004). It has been known that aminopeptidase controls the A $\beta$ -associated protective function physiologically by cleaving N-terminal aspartate residue of amyloid beta (A $\beta$ ) peptides (Ballatore et al. 2007; Sevalle et al. 2009). Aminopeptidase also plays an important role in tauopathies where a group of neurodegenerative disorders were characterized by abnormal accumulation of hyperphosphorylated TAU protein in the form of NFTs (Ballatore et al. 2007). Reduction of TAU helps to develop potential therapy for AD and other tauopathies (Brunden et al. 2009, 2010). Recently, the puromycin-sensitive aminopeptidase (PSA/NPEPPS) ability was studied in vivo in the *Drosophila* model to protect from TAU-induced neurodegeneration (Brunden et al. 2009). Similarly, the role of human PSA/NPEPPS (hPSA) as a TAU aminopeptidase was confirmed in a cell-free system (Brunden et al. 2009). Aminopeptidase initially cleaves at the N-terminus of TAU which is most useful for the aggregation and for TAU-induced neuropathogenesis (Amadoro et al. 2004; Gamblin et al. 2003).

Experimentally, it has been proved that APNs are important in the N-terminal cleavage of A $\beta$  peptides as well as degradation of normal and pathologic tau proteins in AD (Karsten et al. 2006; Sengupta et al. 2006). Similarly, aminopeptidase (SGAK) can also degrade A $\beta$  peptides and inhibit its fibril formation (Yoo et al. 2010). But till now we do not have clear information about the interactive residues of aminopeptidase with A $\beta$  peptide at the atomic level.

Hence, in this study, we predicted three-dimensional structure of aminopeptidase (SGAK) by considering known X-ray crystal structure of aminopeptidase from *Streptomyces griseus* (PDBID: 1CP7.pdb) as a template (Gilboa et al. 2000). Then we investigated the active site residues of aminopeptidase (SGAK) which are important to degrade A $\beta$  peptide. Further, the model generated by MODELLER was docked with three different A $\beta$  peptides. We believe that the predicted model of aminopeptidase (SGAK) and its residues involved in the interactions with A $\beta$  peptide along with zinc ions would be useful to find out new therapeutic strategies in AD treatment.

## Methods

### Software and hardware

Three programs such as SWISS-MODEL (Schwede et al. 2003), Geno3D (Combet et al. 2002) and MODELLER 9v7 (Sali and Blundell 1993) were used to build homology model of aminopeptidase (SGAK). The predicted models were evaluated by PROCHECK (Laskowski et al. 1993), PROSA (Wiederstein and Sippl 2007) and Verify-3D (Eisenberg et al. 1997). Molecular docking was performed with AutoDock 4.2 (Morris et al. 2009). Chimera (Pettersen et al. 2004) and visual molecular dynamics (VMD) (Humphrey et al. 1996) were used for interactive visualization and analysis of molecular structures.

### Sequence alignment and homology modeling

The amino acid sequence of aminopeptidase (SGAK) (Acc. No-ABB40595.1) was extracted from NCBI database (<http://www.ncbi.nlm.nih.gov/>). The BLAST search was performed against PDB database to get suitable template structure showing highest sequence similarity with aminopeptidase (SGAK). The aminopeptidase from *S. griseus* (SGAP) (PDBID 1CP7) (Gilboa et al. 2000) with 1.58 Å resolution was used as a template to build 3D model of aminopeptidase (SGAK). The pair-wise sequence alignment of template sequence (1CP7.pdb) and aminopeptidase (SGAK) sequence was done using EMBOSS program (Rice et al. 2000). Then homology modeling of aminopeptidase (SGAK) was performed by SWISS-MODEL

(Schwede et al. 2003), Geno3D (Combet et al. 2002) and MODELLER9V7 (Sali and Blundell 1993). The steepest descent (SD) energy minimization was done to remove steric clashes (Spoel et al. 2005).

#### Secondary structure analysis and model validation

“Self Optimized Prediction Method” program (SOPMA) was used for secondary structure analysis of aminopeptidase (SGAK). The SOPMA program determines the role of individual amino acid to build secondary structure with their positions (Geourjon and Deléage 1995). The models of aminopeptidase generated through SWISS-MODEL (Schwede et al. 2003), Geno3D (Combet et al. 2002) and MODELLER9V7 (Sali and Blundell 1993) were validated by inspection of the Psi/Phi Ramachandran plot (Lovell et al. 2002) obtained by PROCHECK analysis (Laskowski et al. 1993). The model constructed by MODELLER was finally chosen for further investigations on the basis of geometry and 3D alignment with template structure. The PROSA (Wiederstein and Sippl 2007) test was applied for final model to check for energy criteria. The model compatibility with its sequence was measured by Verify-3D (Eisenberg et al. 1997). The Ramachandran plot for model predicted by MODELLER was obtained through PROCHECK analysis (Laskowski et al. 1993). PDBeFOLD server (Krissinel and Henrick 2004) and chimera (Pettersen et al. 2004) were used for the structure comparison between predicted aminopeptidase model (SGAK) and template structure (1CP7.pdb) (Gilboa et al. 2000).

#### Active site prediction

The crystal structure of aminopeptidase (1CP7.pdb) (Gilboa et al. 2000) was compared with predicted aminopeptidase model (SGAK) for the prediction of active site residues present in model (SGAK). The sequence alignment between aminopeptidase from *S. griseus* (template) (Gilboa et al. 2000) and aminopeptidase (SGAK) (target) was done using EMBOSS program (Rice et al. 2000). The 3D alignment between aminopeptidase from *S. griseus* (template) and aminopeptidase (SGAK) (target) was done using chimera (Pettersen et al. 2004) to compare the active site pocket present in the two structures.

#### Molecular dynamic simulation of aminopeptidase model (SGAK)

Molecular dynamic simulation of aminopeptidase model (SGAK) was performed by Gromacs 4.0.4 program (Spoel et al. 2005) using OPLS-AA force field (Jorgensen et al. 1996; Kaminski et al. 2001). The predicted aminopeptidase

model (SGAK) was used as starting structure for MD simulation. The model was surrounded by total 12,270 SPC-type water molecules (water density 1.0). The system was neutralized with 3 Cl<sup>−</sup> ions. The cubic type of box with 9 Å size was used for MD simulation. The solvated structure was minimized by SD method for 15,000 steps at 300 K temperature and constant pressure. The model was equilibrated for 1 ns period. Then MD was run for 10 ns at constant temperature and pressure. The LINCS algorithm (Hess et al. 1997) was used to constrain the bond length. Periodic boundary conditions were applied to the system. A cutoff of 14 Å was used for van der Waals' interactions. PME switch option was used for electrostatic interactions by 8 and 12 Å cutoffs for short-range and long-range interactions, respectively (Essmann et al. 1995). Structural comparisons between initial and final MD simulated structures were carried out using PDBeFOLD (Krissinel and Henrick 2004). The dynamic runs were then visualized using VMD package (Humphrey et al. 1996). The images after simulation were generated using chimera (Pettersen et al. 2004) and PyMOL. The three-dimensional structure of aminopeptidase was analyzed by various softwares such as RasMol (Sayle and Milner-White 1995) PyMOL (<http://PyMOL.sourceforge.net/>) and Chimera (Pettersen et al. 2004).

#### Molecular docking of aminopeptidase (SGAK) and A $\beta$ peptide

The molecular docking was performed between simulated aminopeptidase (SGAK) model and patch of A $\beta$  peptide [<sup>1</sup>DAEFRHDSGY<sup>10</sup>] from wild-type 1IYT.pdb (Crescenzi et al. 2002) using AutoDock 4.2 (Morris et al. 2009). The Zn ions present in aminopeptidase (SGAK) were parameterized by Amber force field available in AutoDock as per earlier studies of metalloproteases (Irwin et al. 2005; Xin and William 2003; Barage and Sonawane 2013; Barage et al. 2014). To remove hard contacts, the docked complex was then minimized by SD method using Gromacs 4.0.4 (Spoel et al. 2005). Lamarckian genetic algorithm (LGA) has been used in this study. The Auto Grid (Morris et al. 2009) program was used to define active site residues. The grid size was set to 56 × 48 × 48 points with a grid spacing of 0.375 Å centered on the selected flexible residues present in the active site of aminopeptidase. The grid box contains the entire binding site of the aminopeptidase which provides enough space for the translation and rotation to A $\beta$  peptide. Step size of 2 Å for translation and 50° for rotation were chosen and the maximum number of energy evaluation was set to 25,00,000. Thus, ten runs were performed. For each of the ten independent runs, a maximum number of 27,000 GA operations were generated on a single population of 150 individuals. The docked complex which shows lower binding energy has been

selected for further studies. The other two A $\beta$  peptide conformations such as wild-type 1AML.pdb [<sup>1</sup>DAEFRHDSGY<sup>10</sup>] (Sticht et al. 1995) and A2V mutant of 1IYT.pdb [<sup>1</sup>DVEFRHDSGY<sup>10</sup>] (mutation at position 2 Ala to Val) (Fede et al. 2009) were docked with the aminopeptidase (SGAK) by the same protocol mentioned above. Then these docked complexes were used for further studies.

#### Molecular dynamic simulation of docked complexes of aminopeptidase (SGAK) and A $\beta$ peptide

The complex of aminopeptidase (SGAK) and patch of A $\beta$  peptide [<sup>1</sup>DAEFRHDSGY<sup>10</sup>] (wild-type 1IYT.pdb) was used as starting structure for MD simulation. This docked complex was then simulated twice for the period of 30 ns each using two different force fields AMBER99SB-ILDN (Lindorff-Larsen et al. 2010) and OPLS-AA (Jorgensen et al. 1996; Kaminski et al. 2001). The molecular dynamics simulation of docked complex of aminopeptidase (SGAK) and A $\beta$  peptide was done by Gromacs 4.0.4 program (Spoel et al. 2005) using OPLS-AA force field (Jorgensen et al. 1996; Kaminski et al. 2001). The complex was encircled by total 12,390 SPC-type water molecules (water density 1.0). To neutralize the system 4 Na<sup>+</sup> ions were used. The cubic type of box with 9 Å size was used for MD simulation. The MD simulation system contains total 39,033 atoms. The solvated structure was minimized by SD method for 15,000 steps at 300 K temperature and constant pressure. Then the complex was equilibrated for 1 ns period. After equilibration production, MD was run for 30 ns at constant temperature and pressure. The LINCS algorithm (Hess et al. 1997) was used to constrain the bond length. Periodic boundary conditions were applied to the system. PME switch option was used to calculate electrostatic interactions by 8 and 12 Å cutoffs for short-range and long-range interactions, respectively (Essmann et al. 1995).

Further the docked complexes of aminopeptidase (SGAK) with wild-type 1AML.pdb (Sticht et al. 1995) and mutated 1IYT.pdb (mutation at position 2 Ala to Val) (Fede et al. 2009) were simulated by OPLS-AA force field (Jorgensen et al. 1996; Kaminski et al. 2001) by the same protocol as mentioned above to compare the interactions of aminopeptidase with A $\beta$  peptide and zinc ions. The starting and final MD simulated structures were compared with the help of PDBeFOLD (Krissinel and Henrick 2004). The structure and dynamic runs were then visualized using VMD package (Humphrey et al. 1996). The analysis of structures after MD simulation was performed by RasMol (Sayle and Milner-White 1995) and images were generated using Chimera (Pettersen et al. 2004) and PyMOL (<http://PyMOL.sourceforge.net/>).

## Results and discussions

### Secondary structure analysis

The secondary structure analysis of aminopeptidase sequence obtained by SOPMA method showed 30.66 % amino acids in helix, 16.48 % in extended strands, 47.83 % in random coil, and 5.03 % in beta turn regions (Supplementary data Fig. 1). The largest part of protein was occupied by random coil but the total regions of alpha helices and extended strands are found at equal percentage. The total percentage of random coil and beta turn forming regions is small which reveals the good quality of model predicted using aminopeptidase sequence (Accession No ABB40595.1).

### Structure prediction and validation

The alignment between target sequence of aminopeptidase (SGAK) (Acc. No ABB40595.1) and the crystal structure of aminopeptidase (PDB-1CP7) (Gilboa et al. 2000) shows 86 % sequence identity (Fig. 1). Three programs such as SWISS-MODEL (Schwede et al. 2003), Geno3D (Combet et al. 2002) and MODELLER 9V7 (Sali and Blundell 1993) were used to build aminopeptidase (SGAK) model. The predicted model quality was evaluated by PROCHECK (Laskowski et al. 1993), PROSA (Wiederstein and Sippl 2007) and VERIFY-3D (Eisenberg et al. 1997). The model built by MODELLER 9V7 (Sali and Blundell 1993) after evaluation by PROCHECK (Laskowski et al. 1993) shows 91.9 % residues in the most favored regions, 5.7 % residues in allowed regions and 2 % residues in generously allowed regions (supplementary data Fig. 2). Hence, total 99.6 % of residues were present in the favored regions and only 0.4 % of residues are in the outer region which suggests the predicted model is of good quality (supplementary data Fig. 2) (Table 1). The model quality was evaluated by checking Z score of structure obtained through PROSA tool (Wiederstein and Sippl 2007). The PROSA (Wiederstein and Sippl 2007) was used to check whether the input structure gives score similar to the score obtained for native protein structure having similar size. The Z score was −7.4 given by PROSA (Wiederstein and Sippl 2007). Hence, the aminopeptidase (SGAK) structure was within the acceptable range of X-ray and NMR studies (supplementary data Fig. 3a). In PROSA II test, maximum number of residues showed negative interaction energy and very few identified with positive interaction energy which confirms the model quality (supplementary data Fig. 3b). The aminopeptidase model (SGAK) obtained by MODELLER (Sali and Blundell 1993) analyzed by PROCHECK (Laskowski et al. 1993) and PROSA (Wiederstein and Sippl 2007) which showed good results, hence used for



**Fig. 1** Sequence alignment between template (1CP7) and the aminopeptidase model (SGAK). Catalytic residues (red) are shown in yellow box (color figure online)

CLUSTAL 2.1 multiple sequence alignment

```

1CP7_A|PDBID|CHAIN|SEQUENCE  -----APDIPLANVKAHLTQLSTIAANNNGNRAHGRPGYKASVDYVK
aminopeptidase                PASRTAAAPDIPVANVKAHLTQLQSIAANGNRAHGRAGYKASIDYVK
                                *****:*****.:**.:*****.*****:***

1CP7_A|PDBID|CHAIN|SEQUENCE  AKLDAAGYTTTLQQFTSGGATGYNLIANWPGGDPNKVLMAGALDLSVSSG
aminopeptidase                AKLDAAGYTTALQQFTSGGATGYNLIADWPGGDPNQVLMAGSLDLSVTSG
                                *****:*****:*****:*****:*****:***

1CP7_A|PDBID|CHAIN|SEQUENCE  AGINONGSGSAVLETA LAVSRAGYQPKHLRFWWGAELGLIGSKFYV
aminopeptidase                AGINONGSGSAVLETA LAVSRAQLTPDKHLRFWWGAELGLIGSKYYV
                                *****:*****:*****:*****:*****:***

1CP7_A|PDBID|CHAIN|SEQUENCE  NNLPSADRSKLAGYLNEDMI GSPNPGYFVYDDDPVIEKTFKNYFAGLNVP
aminopeptidase                NNLGATERAKLDGYLNEDMI GSPNAGYFVYDDDPVIEQTFKSYFAGLSVP
                                ***.:**.:**.:*****:*****:*****:***

1CP7_A|PDBID|CHAIN|SEQUENCE  TEIETEGDGRSDHAPFKNVGVFVGGFTGAGYTKSAAQAQKWGGTAGQAF
aminopeptidase                TEIETEGDGRSDHAPFKSAGVPVGGFTGASNTKSAAQAQKWGGTAGQSF
                                *****:*****:*****:*****:*****:***

1CP7_A|PDBID|CHAIN|SEQUENCE  DRCYSSCDLSNINDTALDRNSDAAAHAIWTLSSGTGEPPT
aminopeptidase                DRCYSSCDNTANINDTALDRNSDAVAHAIWTLSDATPEPZ
                                *****:*****:*****:*****:*****:***

```

**Table 1** PROCHECK and PROSA evaluation of aminopeptidase models obtained by different programs

S. no	Predicted models of aminopeptidase by different programs	PROCHECK analysis showing residues at various regions				PROSA Z score
		Core (%)	Allowed (%)	Generously (%)	Disallowed (%)	
1	Geno3D model 1	81.3	17.0	1.3	0.4	−6.69
2	Geno3D model 2	79.6	17.9	1.7	0.9	−6.37
3	Geno3D model 3	79.1	17.4	2.1	1.3	−6.51
4	Geno3D model 4	83.0	14.9	1.3	0.9	−6.57
5	Geno3D model 5	81.3	16.6	1.3	0.9	−6.73
6	SWISS-MODEL	88.8	9.9	0.9	0.4	−7.7
7	MODELLER	91.9	5.7	2.0	0.4	−7.4

further studies (Table 1). The VERIFY-3D (Eisenberg et al. 1997) analysis tool was used to find the atomic model (3D) compatibility with its own amino acid sequence (1D). The compatibility score obtained for aminopeptidase model was above zero in the VERIFY-3D (Eisenberg et al. 1997) graph which suggests the side-chain environment acceptability (supplementary data Fig. 4) for aminopeptidase model built by MODELLER (Sali and Blundell 1993). The VERIFY-3D (Eisenberg et al. 1997) showed 0.45 score for the predicted model which is nearer to the template score 0.44 (supplementary data Fig. 4). PDBFOLD (Krissinel and Henrick 2004) program was used to compare the predicted structure of aminopeptidase (SGAK) (Fig. 2) with template structure (1CP7.pdb) (Gilboa et al. 2000). The lower RMSD value (0.28 nm) (Fig. 3a) suggests high similarity between two structures. The comparison between aminopeptidase (SGAK) and template (1CP7.pdb) carried out using Chimera (Pettersen et al. 2004) also shows good similarity (Fig. 3a). The active site residues are found similar in the sequence alignment as well as structure

comparison studies between aminopeptidase (SGAK) and aminopeptidase from *S. griseus* (1CP7.pdb) (Figs. 1, 3b). The active site residues of aminopeptidase from *S. griseus* (1CP7.pdb) (His85, Asp97, Glu131, Glu132, Asp160, His247) exactly matches with the active site residues of aminopeptidase (SGAK) (His93, Asp105, Glu139, Glu140, Asp168, His255). Hence, these active site residues (His93, Asp105, Glu139, Glu140, Asp168 and His255) of aminopeptidase (SGAK) might play an important role in the Aβ peptide degradation as can be seen in Fig. 3b. This model was further used for molecular docking studies to find out the interactions of active site residues of aminopeptidase (SGAK) with Aβ peptide.

Molecular docking and MD simulation studies of docked complex of aminopeptidase model (SGAK) and Aβ peptide

Molecular docking and MD simulation studies have been found useful to understand protein and ligand interactions

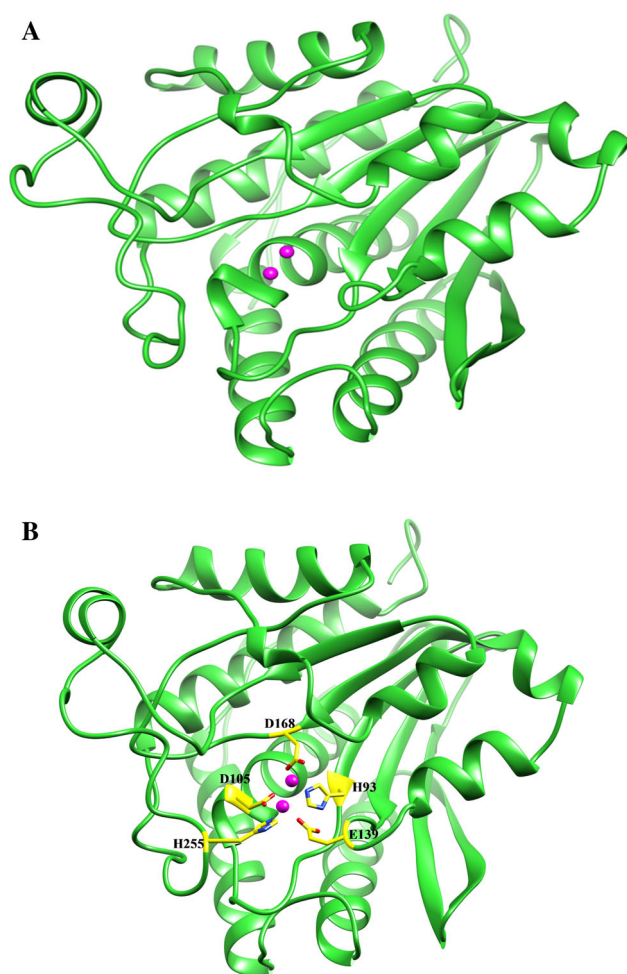


**Fig. 2** **a** Predicted model of aminopeptidase (SGAK) (lime green) with zinc (magenta). **b** Active site residues present in aminopeptidase (SGAK) (yellow) with zinc (magenta) (color figure online)

at the molecular level (Tseng et al. 2007; Jalkute et al. 2013; Barage and Sonawane 2013; Dhanavade et al. 2013; Barage et al. 2014). Hence, molecular docking study was performed using AutoDock 4.2 (Morris et al. 2009) in which the active site residues (His93, Asp105, Glu139, Glu140, Asp168, and His255) of aminopeptidase (SGAK) were kept flexible. This aminopeptidase model was then docked with three different conformations of A $\beta$  peptide (wild-type 1IYT.pdb, wild-type 1AML.pdb and mutated A2V of 1IYT.pdb) [<sup>1</sup>DAEFRHDSGY<sup>10</sup>]. The aminopeptidase (SGAK) complex with wild-type 1IYT.pdb shows strong hydrogen bonding than other two complexes with wild-type 1AML.pdb and A2V mutant of 1IYT.pdb (Tables 2, 3, 4). Hence, the complex of aminopeptidase (SGAK) and wild-type 1IYT.pdb was analyzed further.

This docked complex of aminopeptidase (SGAK) and wild-type 1IYT.pdb shows strong hydrogen bonding between active site residues and A $\beta$  peptide along with zinc ions (Table 2; Fig. 4a, b). The active site residues of

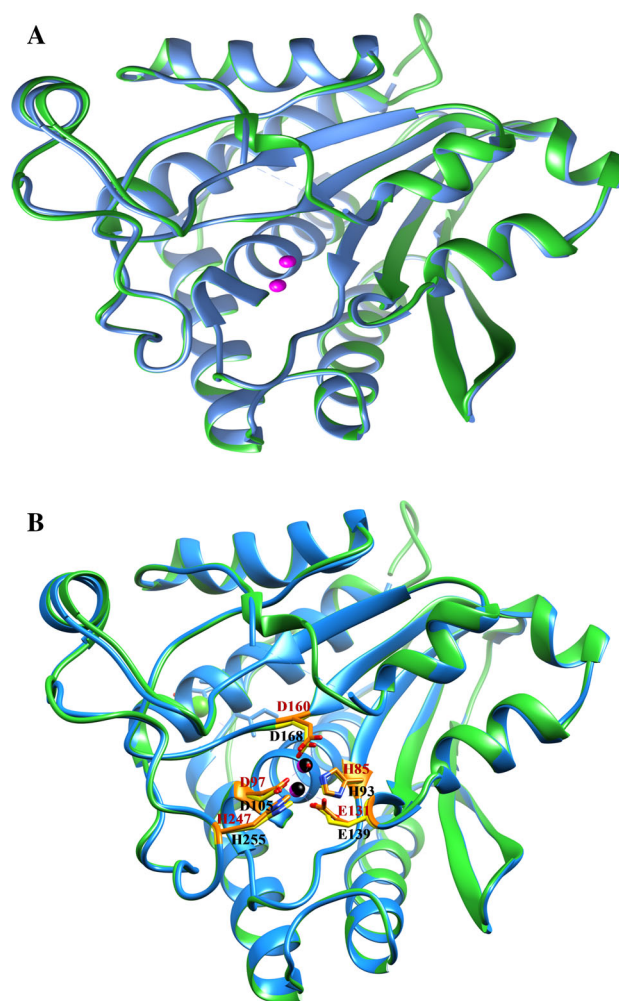


**Fig. 3** **a** Structural comparison between aminopeptidase model (SGAK) (lime green) and template structure (1CP7) (cornflower blue). **b** Active site residue comparison between aminopeptidase (SGAK) (model lime green, active site residues yellow, Zn magenta) and template (1CP7) (structure cornflower blue, active site residues orange, Zn black) (color figure online)

aminopeptidase (SGAK) such as Glu140, Asp168 and His255 interact with Glu3 of A $\beta$  peptide with interatomic distances 2.503, 2.912 and 2.762 Å, respectively. Likewise, His255 of aminopeptidase (SGAK) interacts with Ala2, Phe4 and Arg5 of A $\beta$  peptide by interatomic distances of 1.127, 1.982 and 1.558 Å, respectively (Fig. 4a).

The docked complex of aminopeptidase (SGAK) with wild-type 1IYT.pdb was simulated twice using different force fields OPLS-AA (Jorgensen et al. 1996; Kaminski et al. 2001) and AMBER99SB-ILDN (Lindorff-Larsen et al. 2010) up to 30 ns. The docked complex of aminopeptidase (SGAK) with wild-type 1IYT.pdb simulated by OPLS-AA force field shows strong hydrogen bonding and low average RMSD than the complex simulated by AMBER99SB-ILDN force field (Lindorff-Larsen et al. 2010) (Table 2; Figs. 4, 5, 6, 7a, 8a).

**Table 2** Hydrogen bonding of docked complexes

Interaction between active site residues of aminopeptidase (SGAK) with A $\beta$ peptide and zinc before and MD	Aminopeptidase with 1IYT.pdb before MD (atomic distance in Å)	Aminopeptidase with 1IYT.pdb after OPLS-AA MD (atomic distance in Å)	Aminopeptidase with 1IYT.pdb after AMBER99 SB-ILDN MD (atomic distance in Å)
HIS 255 HE2–ALA 2 O: (A $\beta$ )	1.127	–	–
GLU HE2 (A $\beta$ )–ZN 1	–	1.090	–
HIS 255 HE2–PHE 4 H (A $\beta$ )	1.982	–	–
ASP 168 OD1–GLU 3 H (A $\beta$ )	2.912	2.852	–
GLU 139 OE2–GLU 3 H (A $\beta$ )	2.503	2.328	–
HIS 255 HE2–GLU 3 H (A $\beta$ )	2.762	–	–
HIS 255 HE2–GLU 3 O (A $\beta$ )	–	2.059	–
HIS 255 HD1–ARG 5 H (A $\beta$ )	1.558	–	–
HIS 255 HD1–ARG 5 O (A $\beta$ )	2.212	–	–
GLU 3 O (A $\beta$ )–ZN 2	2.426	1.878	–
ARG 5 O (A $\beta$ )–ZN 2	2.373	–	–
GLU 140 OE2–ZN 2	1.725	1.505	–
GLU 140 OE1–ZN 2	1.765	2.513	2.794
ASP 105 OD1–ZN 1	1.782	2.543	2.781
GLU 139 OE2–ZN 1	1.761	2.718	–
HIS 93 NE2–ZN 1	1.985	–	2.537
HIS 93 HE2–ZN 1	–	2.931	–
ASP 105 OD2–ZN 1	2.594	2.061	–
ASP 105 OD1–ZN 2	2.221	2.125	–
GLU 139 OE1–ZN 2	1.712	2.986	2.894
GLU 139 OE1–ZN 1	2.393	2.277	–
GLU 139 OE2–ZN 2	2.310	2.352	–
ASP 105 OD2–ZN 2	1.715	2.825	2.735
ASP 168 OD1–ZN 1	1.784	2.363	2.652
ASP 168 OD2–ZN 1	1.774	2.610	2.705

**Table 3** Hydrogen bonding between active site residues of aminopeptidase (SGAK) with A $\beta$  peptide (1AML.pdb) and zinc simulated using OPLS-AA force field

Interaction between active site residues of aminopeptidase (SGAK) with A $\beta$ peptide and zinc after MD	Interactions before MD in Å	Interactions after OPLS MD in Å
HIS 255 NE2–ZN 2	2.571	2.625
GLU 140 OE2–ZN 2	2.392	2.574
GLU 140 OE1–ZN 2	2.143	2.358
ASP 105 OD1–ZN 2	2.329	2.546
ASP 105 OD2–ZN 1	2.816	–
GLU 139 OE1–ZN 1	2.776	2.862
HIS 93 NE2–ZN 1	2.773	2.942
ASP 168 OD2–ZN 1	2.348	2.384
ASP 168 OD1–ZN 1	2.377	2.478
GLU 3 H (A $\beta$ )–ZN 1	2.283	2.872
GLU 3 H (A $\beta$ )–ASP 168 OD2	2.623	2.756

**Table 4** Hydrogen bonding between active site residues of aminopeptidase (SGAK) with mutated 1IYT.pdb (mutation at 2 from Ala to Val) and zinc simulated using OPLS-AA force field

Interaction between active site residues of aminopeptidase (SGAK) with mutated 1IYT.pdb and zinc after MD	Interactions before MD in Å	Interactions after OPLS MD in Å
HIS 255 NE2–ZN 2	2.329	2.563
GLU 140 OE1–ZN 2	2.031	2.228
GLU 140 OE2–ZN 2	1.882	2.010
GLU 139 OE1–ZN 1	1.299	1.862
ASP 105 OD2–ZN 1	2.283	2.306
ASP 105 OD1–ZN 2	2.277	2.324
ASP 168 OD1–ZN 1	2.478	2.574
ASP 168 OD2–ZN 1	2.274	2.318
HIS 93 NE2–ZN 1	2.536	2.759
PHE 4 O (A $\beta$ )–ZN 1	2.314	2.430

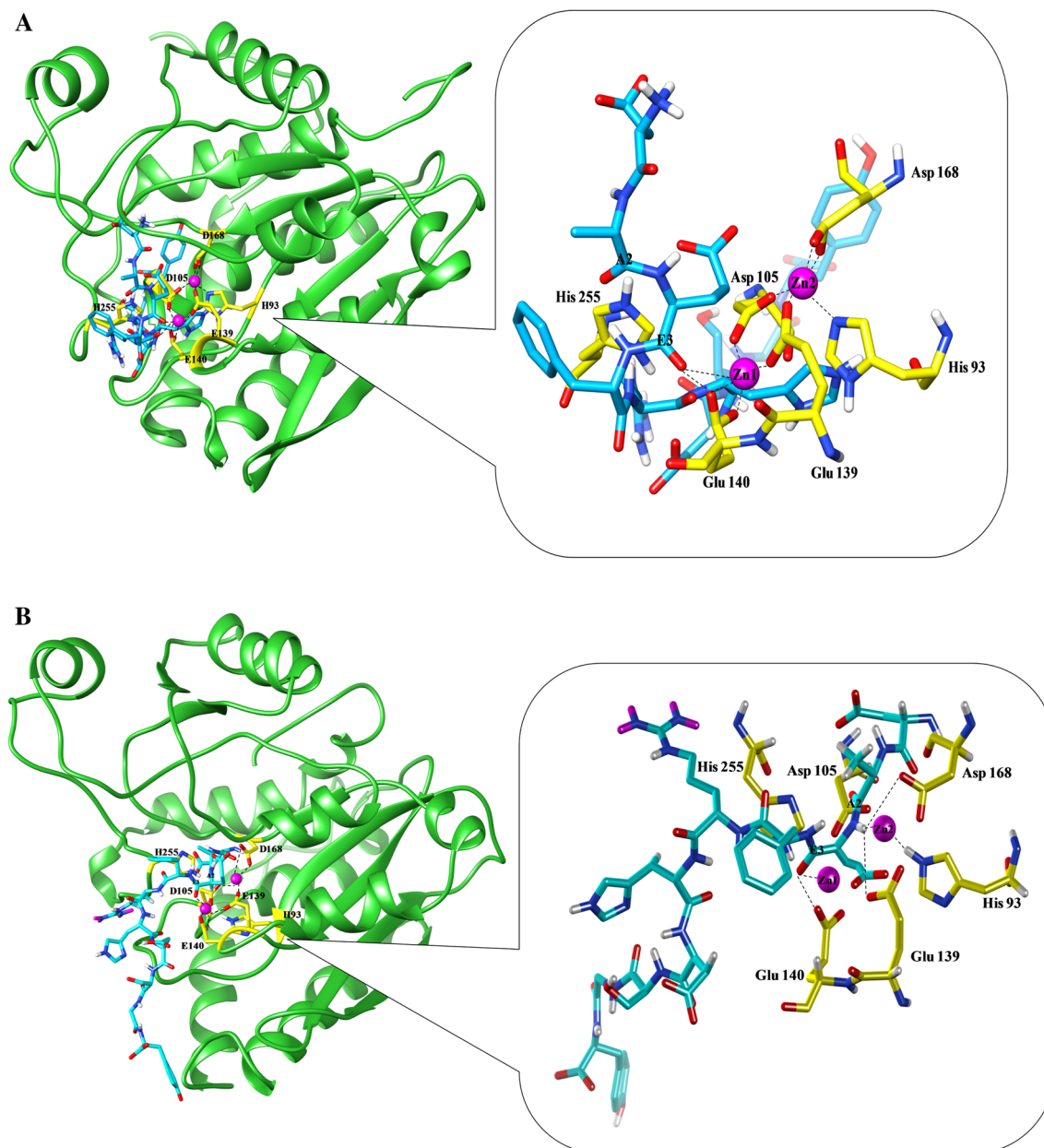


**Fig. 4** Docked complex of aminopeptidase model (SGAK) (lime green) showing hydrogen bonding interactions between active site residues (yellow) with zinc (magenta) and A $\beta$  peptide (cyan). **a** Before MD and **b** after MD simulation (color figure online)

The docked complex of aminopeptidase (SGAK) with wild-type 1IYT.pdb simulated by OPLS-AA force field shows stable behavior up to 30 ns simulation period (Fig. 6). The average RMSD value of simulated docked complex of aminopeptidase (SGAK) with wild-type 1IYT.pdb by OPLS-AA force field (Jorgensen et al. 1996; Kaminski et al. 2001) was 0.29 nm (Fig. 6), whereas by AMBER99SB-ILDN force field (Lindorff-Larsen et al. 2010) it was 0.33 nm (Fig. 8a). Hence, the docked complex of aminopeptidase (SGAK) with wild-type 1IYT.pdb simulated by OPLS-AA force field (Jorgensen et al. 1996;

Kaminski et al. 2001) was more stable than the complex simulated by AMBER99SB-ILDN force field (Lindorff-Larsen et al. 2010) (Figs. 6, 8a).

The docked complex of aminopeptidase (SGAK) with wild-type 1IYT.pdb has also been compared with two different docked complexes such as aminopeptidase (SGAK) with wild-type 1AML.pdb and aminopeptidase (SGAK) with A2V mutant of 1IYT.pdb. The docked complex of aminopeptidase (SGAK) with wild-type 1AML.pdb shows less hydrogen bonding and high average RMSD (0.34 nm) (Tables 2, 3; Figs. 4, 5, 6, 7b, 8b).



Similarly, docked complex of aminopeptidase (SGAK) with mutated 1IYT.pdb also shows less interactions and high average RMSD (0.33 nm) (Tables 2, 4; Figs. 4, 5, 6, 7c, 8c) as compared to docked complex of aminopeptidase (SGAK) with wild-type 1IYT.pdb which shows strong hydrogen bonding and low average RMSD (0.29 nm) (Table 2; Figs. 4b, 5, 6).

Hence, docked complex of aminopeptidase (SGAK) with wild-type 1IYT.pdb was studied further. The hydrogen bonding between active site residues Glu140, Asp168 and His255 of aminopeptidase (SGAK) with Glu3 of A $\beta$  peptide (wild-type 1IYT.pdb) was 2.628, 2.852 and 2.059 Å, respectively (Fig. 4b). These interactions were maintained throughout the MD simulation done by OPLS-

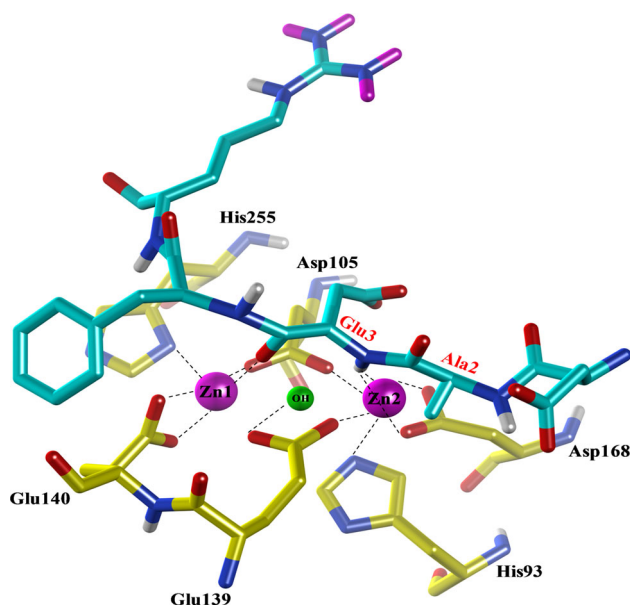
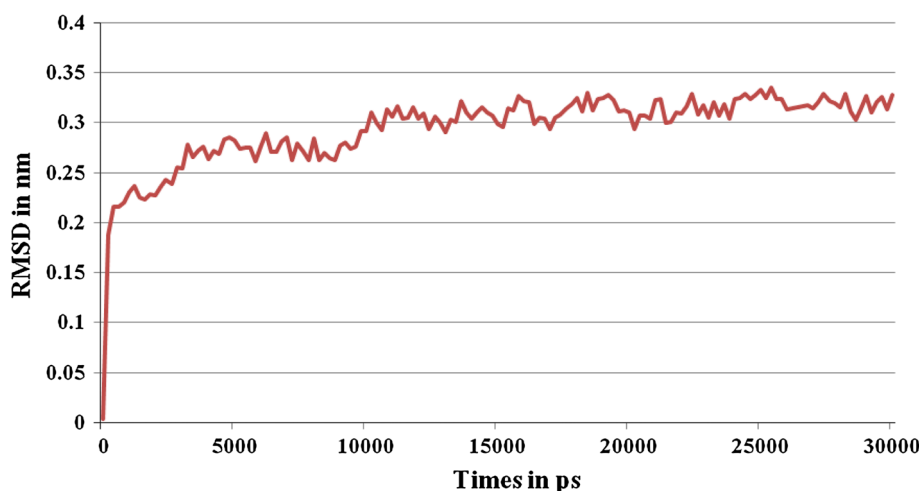


**Fig. 5** Interaction between active site residues (yellow) of aminopeptidase (SGAK) (lime green) with A $\beta$  peptide (cyan) and zinc (magenta) (color figure online)

**Fig. 6** RMSD of docked complex of aminopeptidase (SGAK) and 1IYT.pdb



AA force field (Fig. 4b; Table 2) suggesting that aminopeptidase (SGAK) might cleave A $\beta$  peptide between Ala2 and Glu3. Earlier, experimental results suggest that the aminopeptidase (SGAK) cleaves A $\beta$  peptide from first (D) up to tenth (Y) amino acid successively (Yoo et al. 2010). Our molecular docking study revealed that the aminopeptidase (SGAK) cleaves A $\beta$  peptide at Glu3 similar to experimental findings (Yoo et al. 2010).

The MD simulated stable structure of aminopeptidase was docked with A $\beta$  peptide. This docked complex was simulated for 30 ns. The average RMSD value of docked complex of aminopeptidase (SGAK) and A $\beta$  peptide was 0.29 nm which indicates stable behavior of docked complex up to 30 ns simulation period (Fig. 6). Radius of gyration (Rg) also showed stable behavior during simulation period (Fig. 9). The RMSF for C-alpha depicts small fluctuations for the rigid structural elements and larger fluctuations at the end and loops (Fig. 10). All these results revealed that the docked complex of aminopeptidase (SGAK) and A $\beta$  peptide was stable throughout the 30 ns simulation period.

#### Interactions between active site residues of aminopeptidase (SGAK) with A $\beta$ peptide

The active site of aminopeptidase (SGAK) has two Zn<sup>2+</sup> ions coordinated by histidine, glutamate and aspartate residues (Figs. 5, 11, 12, 13) similar to aminopeptidase from *S. griseus* (1CP7.pdb) (Gilboa et al. 2000). Both the Zn<sup>2+</sup> ions show tetrahedral coordination geometry (Fig. 13). The active site residues (His93, Asp105, Glu139, Glu140, Asp168 and His255) of aminopeptidase (SGAK) exactly match with active site residues (His97, ASP117, Glu151, Glu152, ASP179 and His256) of aminopeptidase from *Aeromonas proteolytica* (Schurer et al. 2004). The cleavage mechanism of aminopeptidase from *A.*

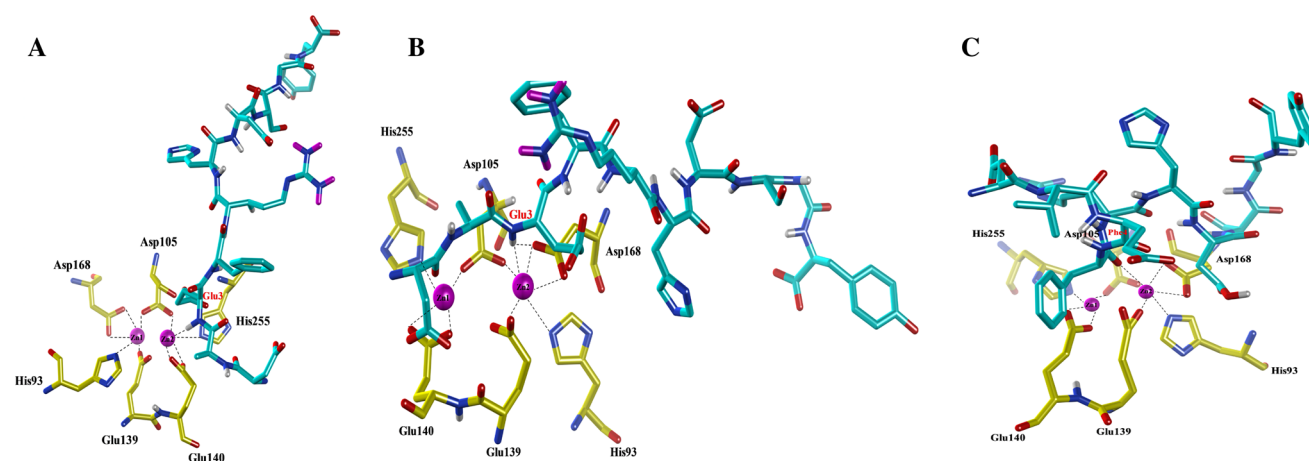


**Fig. 7** Interaction between active site residues (yellow) of aminopeptidase (SGAK) with **a** IYT.pdb (cyan) and zinc (magenta) simulated by AMBER99SBILDN force field. **b** 1AML.pdb (cyan)

and zinc (magenta) simulated using OPLS-AA force field. **c** Mutated 1IYT.pdb (cyan) and zinc (magenta) simulated using OPLS-AA force field (color figure online)

**Fig. 8** The average RMSD of **a** docked complex of Aminopeptidase (SGAK) with IYT.pdb simulated by AMBER99SBILDN force field. **b** Docked complex of aminopeptidase (SGAK) with 1AML.pdb simulated using OPLS-AA force field. **c** Docked complex of aminopeptidase (SGAK) with mutated 1IYT.pdb simulated using OPLS-AA force field

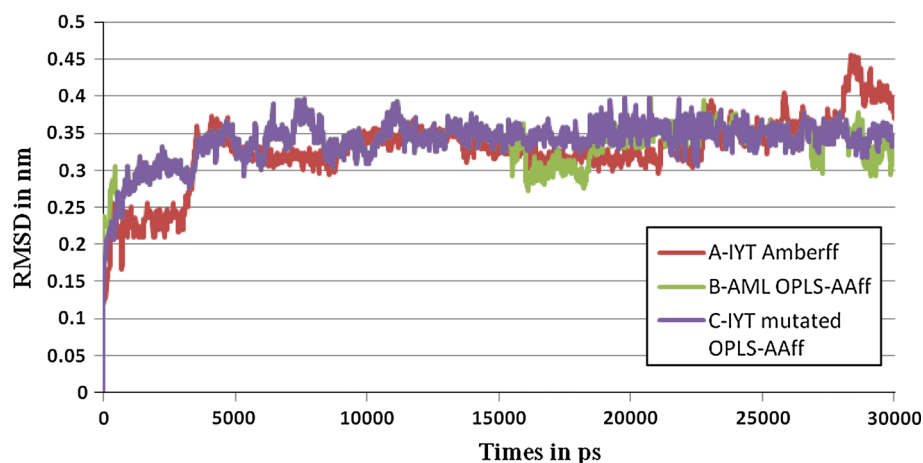
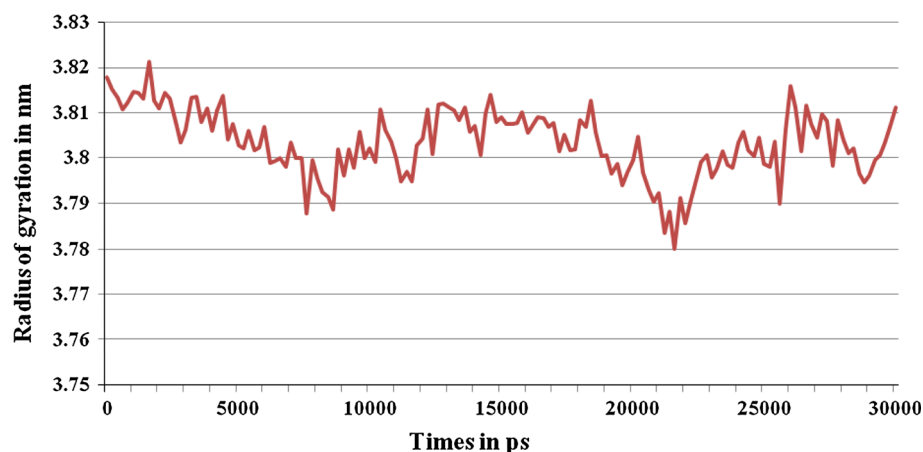


**Fig. 9** Radius of gyration of docked complex of aminopeptidase (SGAK) and A $\beta$  peptide (IYT.pdb) simulated using OPLS-AA force field



*proteolytica* has already been studied previously (Chen et al. 1997; Stamper et al. 2001; Schurer et al. 2004). The MD simulation studies of docked complex of aminopeptidase (SGAK) with A $\beta$  peptide (wild-type 1IYT.pdb)

revealed that the water molecule was closer to Glu139 along with zinc surface and placed properly to attack on the scissile peptide bond between Ala2 and Glu3 of A $\beta$ -peptide similarly as observed for residue Glu151 of aminopeptidase

**Fig. 10** RMSF of docked complex of aminopeptidase (SGAK) and A $\beta$  peptide (IYT.pdb) simulated using OPLS-AA force field

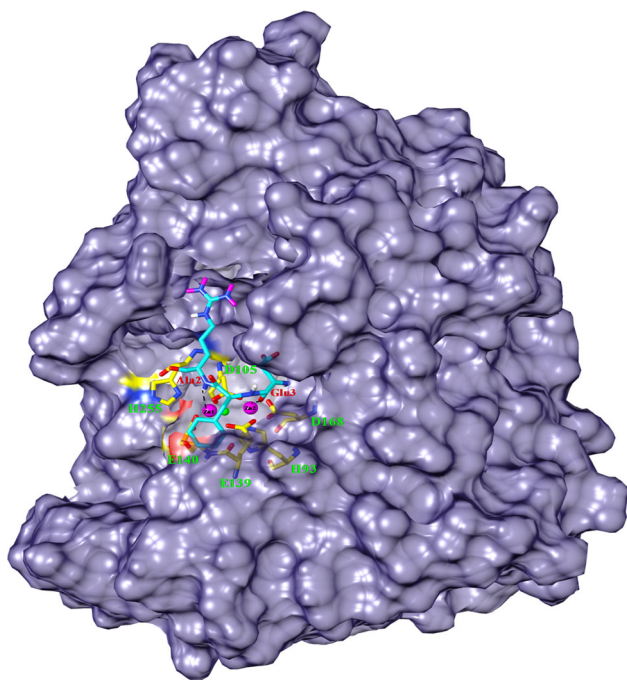
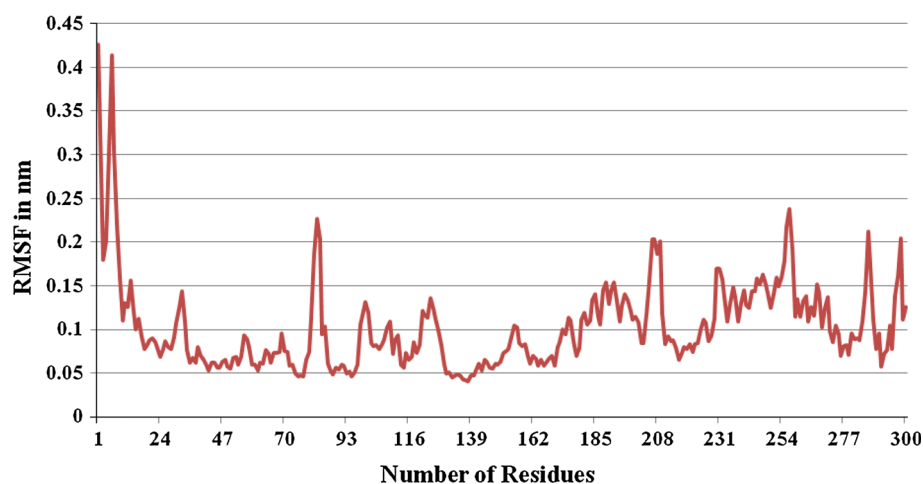


**Fig. 11** A $\beta$  peptide (cyan) binds to aminopeptidase (SGAK) (medium purple) with its active site residues (yellow) labeled with lime green (color figure online)

from *Aeromonas proteolytica* (Schurer et al. 2004) (Fig. 5). The residue Asp105 of aminopeptidase (SGAK) and water molecule or hydroxide ion bridges the two zinc ions. Hence, these residues along with water molecule might play a crucial role in enzyme catalysis of aminopeptidase to cleave A $\beta$  peptide which may be further confirmed by QM/MM studies. The Glu151 acts as a general base in the catalytic mechanism of aminopeptidase from *Aeromonas proteolytica* (Schurer et al. 2004). The residue Glu139 of aminopeptidase (SGAK) shows similarity to Glu151 of aminopeptidase from *A. proteolytica* present in the active site hence it may act as a general base in the catalytic

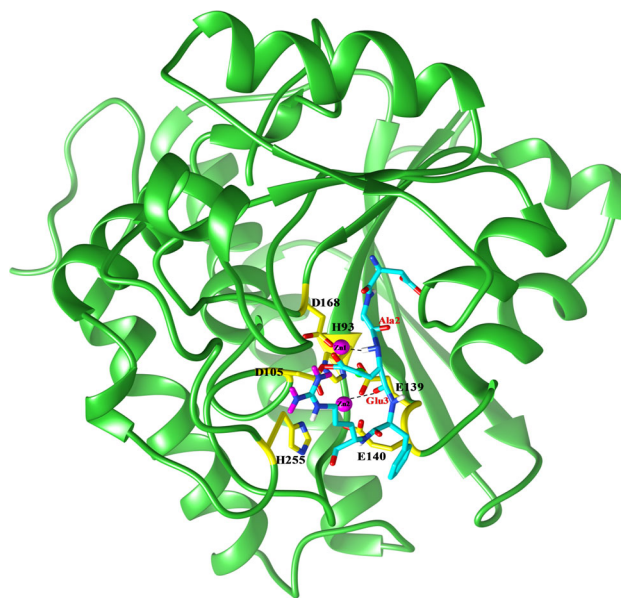
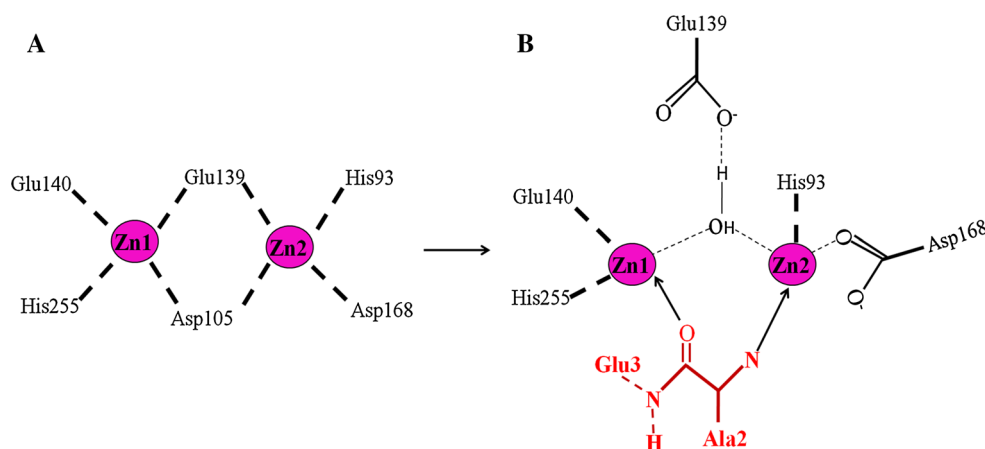


**Fig. 12** Docked complex showing interaction between active site residues (yellow) of aminopeptidase (SGAK) (lime green) with A $\beta$  peptide (cyan) and zinc (magenta) (color figure online)

reaction (Chevrier et al. 1996). This Glu139 remained hydrogen bonded to bridging water molecule. The A $\beta$  peptide binds to Zn2 with N-terminal amino group and to Zn1 with the carbonyl oxygen of the scissile peptide bond of Al2–Glu3. The N-terminus also interacts with the Asp168. After A $\beta$  peptide binds to enzyme, the bridging water molecule loses its coordination to Zn2 and becomes terminally bound to Zn1 similar to aminopeptidase from *Aeromonas proteolytica* (Schurer et al. 2004). This type of carboxylate–histidine metal triads has been observed in the different Zinc-containing enzymes (Christianson and Alexander 1989). Hence, interactive residues Glu139, Asp105 and Asp168 of aminopeptidase (SGAK) with zinc and A $\beta$  peptide may be important to design new therapeutic approach in the AD treatment.

**Fig. 13** Residues involved in the cleavage mechanism of A $\beta$  peptide by aminopeptidase (SGAK). **a** Zinc coordinates of active site residues of aminopeptidase (SGAK). **b** The active site residues interacting with zinc (magenta) and A $\beta$  peptide (shown in red) (color figure online)



## Conclusion

Sequence analysis and model comparison results revealed that active site residues of aminopeptidase (SGAK) are exactly similar to the active site residues of aminopeptidase from *S. griseus* (1CP7.pdb). The docked complex of aminopeptidase with wild-type 1IYT.pdb found more stable as compared to docked complexes of aminopeptidase with wild-type 1AML.pdb and A2V mutant of 1IYT.pdb. The interactions between aminopeptidase (SGAK) active site residues such as Glu140, Asp168 and His255 with amino terminal Ala2–Glu3 of A $\beta$  peptide were maintained throughout MD simulation which suggests their involvement to degrade A $\beta$  peptides. The molecular docking and MD simulation results showed that the aminopeptidase (SGAK) residues could cleave A $\beta$  peptides in between Ala2–Glu3 similar to aminopeptidase from *Aeromonas proteolytica* (Schurer et al. 2004). The residue Glu139 might play an important role in the catalytic mechanism to degrade A $\beta$  peptides. Additional stability to the complex may occur due to interactions between His255 of aminopeptidase with Ala2, Phe4 and Arg5 of A $\beta$  peptide. Hence, the predicted three-dimensional structure of aminopeptidase (SGAK) could be useful to understand the cleavage mechanism of A $\beta$  peptide degradation as well as to design new lead structures to combat AD.

**Acknowledgments** MJD is thankful to Department of Science and Technology, New Delhi for providing fellowship as research assistance under the scheme DST-PURSE. KDS is thankful to the Department of Biotechnology, New Delhi for financial support under the scheme DBT-IPLS sanctioned to Shivaji University, Kolhapur. Authors are thankful to Computer Centre, Shivaji University, Kolhapur for providing the computational facility.

**Conflict of interest** All authors have no conflict of interest.

## References

- Amadoro G, Serafino AL, Barbato C, Ciotti MT, Sacco A, Calissano P, Canu N (2004) Role of N-terminal tau domain integrity on the survival of cerebellar granule neurons. *Cell Death Differ* 11:217–230
- Ballatore C, Lee VM, Trojanowski JQ (2007) Tau-mediated neurodegeneration in Alzheimer's disease and related disorders. *Nat Rev Neurosci* 8:663–672
- Barage SH, Sonawane KD (2013) Exploring mode of phosphoramidon and A $\beta$  peptide binding to hECE-1 by molecular dynamics and docking studies. *Protein Pept Lett* 21:140–152
- Barage SH, Jalkute CB, Dhanavade MJ, Sonawane KD (2014) Simulated interactions between endothelin converting enzyme and A $\beta$  peptide: insights into subsite recognition and cleavage mechanism. *Int J Pept Res Ther*. doi:10.1007/s10989-014-9403-2
- Brunden KR, Trojanowski JQ, Lee VM (2009) Advances in tau-focused drug discovery for Alzheimer's disease and related tauopathies. *Nat Rev Drug Discov* 8:783–793
- Brunden KR, Ballatore C, Crowe A, Smith AB 3rd, Lee VM, Trojanowski JQ (2010) Tau-directed drug discovery for Alzheimer's disease and related tauopathies: a focus on tau assembly inhibitors. *Exp Neurol* 223:304–310
- Chen G, Edwards T, D'souza V, Holz RC (1997) Mechanistic studies on the aminopeptidase from *Aeromonas proteolytica*: a two-metal ion mechanism for peptide hydrolysis. *Biochemistry* 36:4278–4286
- Chevrier B, D'Orchymont H, Schalk C, Tarnus C, Moras D (1996) The structure of the *Aeromonas proteolytica* aminopeptidase complexed with a hydroxamate inhibitor. *Eur J Biochem* 237:393–398
- Christianson DW, Alexander RS (1989) Carboxylate–histidine–zinc interactions in protein structure and function. *J Am Chem Soc* 111:6412–6419
- Combet C, Jambon M, Deléage G, Geourjon C (2002) Geno3D: automatic comparative molecular modelling of protein. *Bioinformatics* 18:213–214
- Crescenzi O, Tomaselli S, Guerrini R, Salvadori S, D'Urso AM, Temussi PA, Picone D (2002) Solution structure of the Alzheimer amyloid beta-peptide (1–42) in an apolar microenvironment similarity with a virus fusion domain. *Eur J Biochem* 269(22):5642–5648



- Dhanavade MJ, Jalkute CB, Barage SH, Sonawane KD (2013) Homology modeling, molecular docking and MD simulation studies to investigate role of cysteine protease from *Xanthomonas campestris* in degradation of A $\beta$  peptide. *Comput Biol Med* 43:2063–2070
- Eisenberg D, Luthy R, Bowie JU (1997) VERIFY3D: assessment of protein models with three-dimensional profiles. *Methods Enzymol* 277:396–404
- Essmann U, Perera L, Berkowitz ML, Darden T, Lee H, Pedersen LG (1995) A smooth particle mesh Ewald method. *J Chem Phys* 103:8577–8593
- Fede GD et al (2009) A recessive mutation in the APP gene with dominant-negative effect on amyloidogenesis. *Science* 323(5920):1473–1477
- Gamblin TC, Chen F, Zambrano A, Abraha A, Lagalwar S, Guillozet AL, Lu M, Fu Y, Garcia-Sierra F, LaPointe N et al (2003) Caspase cleavage of tau: linking amyloid and neurofibrillary tangles in Alzheimer's disease. *Proc Natl Acad Sci USA* 100:10032–10037
- Geourjon C, Deléage G (1995) SOPMA: significant improvements in protein secondary structure prediction by consensus prediction from multiple alignments. *Comput Appl Biosci* 11(6):681–684
- Gilboa R, Greenblatt HM, Perach M, Spungin-Bialik A, Lessel U, Wohlfahrt G, Schomburg D, Blumberg S, Shohama G (2000) Interactions of *Streptomyces griseus* aminopeptidase with a methionine product analogue: a structural study at 1.53 Å resolution. *Acta Cryst D* 56:551–558
- Gonzales T, Robert-Baudouy J (1996) Bacterial aminopeptidases: properties and functions. *FEMS Microbiol Rev* 18:319–344
- Haass C, Selkoe DF (2007) Soluble protein oligomers in neurodegeneration: lessons from the Alzheimer's amyloid beta-peptide. *Nat Rev Mol Cell Biol* 8:101–112
- Hess B, Bekker H, Berendsen HJC, Fraaije JGEM (1997) LINCS: a linear constraint solver for molecular simulations. *J Comput Chem* 18:1463–1472
- Hui KS (2007) Neuropeptidases. In: Lajtha A, Banik NL (eds) *Handbook of neurochemistry and molecular neurobiology: neural protein metabolism and function*, vol 7, 3rd edn. Springer, New York, USA
- Humphrey W, Dalke A, Schulten K (1996) VMD: visual molecular dynamics. *J Mol Graph* 14:33–38
- Irwin JJ, Raushel FM, Shoichet BK (2005) Virtual screening against metalloenzymes for inhibitors and substrates. *Biochemistry* 44:12316–12328
- Iwatsubo T, Saido TC, Mann DM, Lee VMY, Trojanowski JQ (1996) Full-length amyloid- $\beta$  (1–42(43)) and amino-terminally modified and truncated amyloid  $\beta$ 42(43) deposit in diffuse plaques. *Am J Pathol* 149:1823–1830
- Jalkute CB, Barage SH, Dhanavade MJ, Sonawane KD (2013) Molecular dynamics simulation and molecular docking studies of angiotensin converting enzyme with inhibitor lisinopril and amyloid beta peptide. *Protein J* 32:356–364
- Jorgensen WL, Maxwell DS, TiradoRives J (1996) Development and testing of the OPLS all-atom force field on conformational energetics and properties of organic liquids. *J Am Chem Soc* 118:11225–11236
- Kaminski GA, Friesner RA, Tirado-Rives J, Jorgensen WL (2001) Evaluation and reparametrization of the OPLS-AA force field for proteins via comparison with accurate quantum chemical calculations on peptides. *J Phys Chem B* 105:6474–6487
- Karsten SL, Sang TK, Gehman LT, Chatterjee S, Liu J, Lawless GM, Sengupta S, Berry RW, Pomakian J, Oh HS et al (2006) A genomic screen for modifiers of tauopathy identifies puromycin-sensitive aminopeptidase as an inhibitor of tau-induced neurodegeneration. *Neuron* 51:549–560
- Krissinel E, Henrick K (2004) Secondary-structure matching (SSM), a new tool for fast protein structure alignment in three dimensions. *Acta Crystallogr D* 60:2256–2268
- Laskowski RA, McArthur MW, Moss DS, Thornton JM (1993) PROCHECK a program to check stereo-chemical quality of a protein structures. *J Appl Crystallogr* 26:283–291
- Lendeckel U, Arndt M, Frank K, Spiess A, Reinhold D, Ansorge S (2000) Modulation of WNT-5A expression by actinonin: linkage of APN to the WNT-pathway? *Adv Exp Med Biol* 477:35–41
- Lindorff-Larsen K et al (2010) Improved side-chain torsion potentials for the amber ff99SB protein force field. *Proteins* 78:1950–1958
- Lovell SC, Davis IW, Arendall WB, de Bakker PIW, Word JM, Prisant MG, Richardson JS, Richardson DC (2002) Structure validation by C alpha geometry: phi, psi and C beta deviation. *Proteins* 50:437–450
- Miller CG, Green L (1983) Degradation of proline peptides in peptidase-deficient strains of *Salmonella typhimurium*. *J Bacteriol* 153:350–356
- Morris GM, Huey R, Lindstrom W, Sanner MF, Belew RK, Goodsell DS, Olson AJ (2009) AutoDock4 and AutoDockTools4: automated docking with selective receptor flexibility. *J Comput Chem* 30:2785–2791
- Pettersen EF, Goddard TD, Huang CC, Couch GS, Greenblatt DM, Meng EC, Ferrin TE (2004) UCSF Chimera—a visualization system for exploratory research and analysis. *J Comput Chem* 25:1605–1612
- Reeve CA, Bockman AT, Matin A (1984) Role of protein degradation in the survival of carbon-starved *Escherichia coli* and *Salmonella typhimurium*. *J Bacteriol* 157:758–763
- Rice P, Longden I, Bleasby A (2000) EMBOS: the European molecular biology open software suite. *Trends Genet* 16(6):276–277
- Sali A, Blundell TL (1993) Comparative protein modelling by satisfaction of spatial restraints. *J Mol Biol* 234:779–815
- Sarah MS, Yungui Z, Hideaki A, Roberson ED, Sun B, Chen J, Wang X, Yu G, Esposito L, Lennart M, Gan Li (2006) Anti-amyloidogenic and neuroprotective functions of cathepsin B: implications for Alzheimer's disease. *Neuron* 51:703–714
- Sayle RA, Milner-White EJ (1995) RASMOL: biomolecular graphics for all. *Trends Biochem Sci* 20(9):374
- Schurer G, Lanig H, Clark T (2004) *Aeromonas proteolytica* aminopeptidase: an investigation of the mode of action using a quantum mechanical/molecular mechanical approach. *Biochemistry* 43:5414–5427
- Schwede T, Kopp J, Guex N, Peitsch MC (2003) SWISS-MODEL: an automated protein homology-modeling server. *Nucleic Acids Res* 31:3381–3385
- Selkoe DJ (1991) The molecular pathology of Alzheimer's disease. *Neuron* 6:487–498
- Selkoe DF (2004) Cell biology of protein misfolding: the examples of Alzheimer's and Parkinson's diseases. *Nat Cell Biol* 6:1054–1061
- Selkoe DF, Wolfe M (2007) Presenilin: running with scissors in the membrane. *Cell* 131:215–221
- Sengupta S, Horowitz PM, Karsten SL, Jackson GR, Geschwind DH, Fu Y, Berry RW, Binder LI (2006) Degradation of tau protein by puromycin-sensitive aminopeptidase in vitro. *Biochemistry* 45:15111–15119
- Sevalle J, Amoyel A, Robert P, Fournie-Zaluski MC, Roques B, Checler F (2009) Aminopeptidase A contributes to N-terminal truncation of amyloid  $\beta$ -peptide. *J Neurochem* 109:248–256
- Spoel VD, Lindahl E, Hess B, Groenhof G, Mark AE, Berendsen HJ (2005) GROMACS: fast, flexible, and free. *J Comput Chem* 26(16):1701–1718
- Stamper C, Bennett B, Edwards T, Holz RC, Ringe D, Petsko G (2001) Inhibition of the aminopeptidase from *Aeromonas*

- proteolytica* by L-leucinephosphonic acid. Spectroscopic and crystallographic characterization of the transition state of peptide hydrolysis. *Biochemistry* 40:7035–7046
- Sticht H, Bayer P, Willbold D, Dames S, Hilbich C, Beyreuther K, Frank RW, Rosch P (1995) Structure of amyloid A4-(1–40)-peptide of Alzheimer's disease. *Eur J Biochem* 233:293–298
- Stoltze L, Schirle M, Schwarz G, Schroter C, Thompson MW, Hersh LB, Kalbacher H, Stevanovic S, Rammensee HG, Schild H (2000) Two new proteases in the MHC class I processing pathway. *Nat Immunol* 1:413–418
- Takeda A, Araki W, Akiyama H, Tabira T (2004) Amino-truncated amyloid b-peptide (Ab5–40/42) produced from caspase-cleaved amyloid precursor protein is deposited in Alzheimer's disease brain. *FASEB J* 18:1755–1757
- Tanzi RE, Moir RD, Wagner SL (2004) Clearance of Alzheimer's A beta peptide: the many roads to perdition. *Neuron* 43:605–608
- Taylor A (1993a) Aminopeptidases: structure and function. *FASEB J* 7:290–298
- Taylor A (1993b) Aminopeptidases: towards a mechanism of action. *Trends Biochem Sci* 18:167–171
- Tekirian TL, Saido TC, Markesbery WR, Russell MJ, Wekstein DR, Patel E, Geddes JW (1998) N-terminal heterogeneity of parenchymal and cerebrovascular A beta deposit. *J Neuropathol Exp Neurol* 57:76–94
- Thal DR, Sassin I, Schultz C, Haass C, Braak E, Braak H (1999) Fleecy amyloid deposits in the internal layers of the human entorhinal cortex are comprised of N-terminal truncated fragments of A beta. *J Neuropathol Exp Neurol* 58:210–216
- Tseng G, Sonawane KD, Korolkova YV, Zhang M, Liu J, Grishin EV, Guy RH (2007) Probing the outer mouth structure of the HERG channel with peptide toxin footprinting and molecular modeling. *Biophys J* 92:3524–3540
- Wiederstein M, Sippl MJ (2007) ProSA-web: interactive web service for the recognition of errors in three-dimensional structures of proteins. *Nucleic Acids Res* 35:W407–W410
- Xin H, William HS (2003) Docking studies of matrix metalloproteinase inhibitors: zinc parameter optimization to improve the binding free energy prediction. *J Mol Graph Model* 22:115–126
- Yao T, Cohen RE (1999) Giant proteases: beyond the proteasome. *Curr Biol* 9:R551–R553
- Yoo C, Ahn K, Park JE, Kim MJ, Jo SA (2010) An aminopeptidase from *Streptomyces* sp. KK565 degrades beta amyloid monomers, oligomers and fibrils. *FEBS Lett* 584:4157–4162